ChemMedChem

Research Article
doi.org/10.1002/cmdc.202300015

Check for updates

Chemistry
Europe
European Chemical
Societies Publishing

www.chemmedchem.org

Synthesis and Anti-*Mycobacterium tuberculosis* Activity of Imidazo[2,1-*b*][1,3]oxazine Derivatives against Multidrug-Resistant Strains

Guilherme F. S. Fernandes[+],*[a, b, d] Karyn F. Manieri[+],[a] Andressa F. Bonjorno,[a] Debora L. Campos,[a] Camila M. Ribeiro,[a] Fernanda M. Demarqui,[a] Daniel A. G. Ruiz,[c] Nailton M. Nascimento-Junior,[c] William A. Denny,[b] Andrew M. Thompson,*[b] Fernando R. Pavan,*[a] and Jean L. Dos Santos*[a]

The emergence of multidrug-resistant strains of *M. tuberculosis* has raised concerns due to the greater difficulties in patient treatment and higher mortality rates. Herein, we revisited the 2-nitro-6,7-dihydro-5*H*-imidazo[2,1-*b*][1,3]oxazine scaffold and identified potent new carbamate derivatives having MIC_{90} values of 0.18–1.63 μM against *Mtb* H37Rv. Compounds **47–49**, **51–53**, and **55** exhibited remarkable activity against a panel of clinical isolates, displaying MIC_{90} values below 0.5 μM. In *Mtb*-infected macrophages, several compounds demonstrated a 1-log greater reduction in mycobacterial burden than rifampicin and pretomanid. The compounds tested did not exhibit significant cytotoxicity against three cell lines or any toxicity to *Galleria mellonella*. Furthermore, the imidazo[2,1-*b*][1,3]oxazine derivatives did not show substantial activity against other bacteria or fungi. Finally, molecular docking studies revealed that the new compounds could interact with the deazaflavin-dependent nitroreductase (Ddn) in a similar manner to pretomanid. Collectively, our findings highlight the chemical universe of imidazo[2,1-*b*][1,3]oxazines and their promising potential against MDR-TB.

Introduction

Even ~11,000 years after the first known case of tuberculosis (TB), the disease remains one of the greatest threats to global public health.[1,2] TB is the second leading cause of death from an infectious agent, behind only COVID-19.[3] According to the latest report by the World Health Organization (WHO), TB was responsible for the deaths of 1.4 million people worldwide in 2021.[3] In comparison, COVID-19 was responsible for the deaths of 3.5 million people in the same year.[4] Among these deaths from TB, 191,000 were caused by resistant strains of *Mycobacterium tuberculosis* (*Mtb*).[3] Drug-resistant forms of the disease (DR-TB) are currently the main challenge for health authorities and the scientific community in the fight against TB.[5–7] Currently, there are 3 classifications for DR-TB: i) multidrug or rifampicin (RIF)-resistant TB (MDR/RR-TB), classified as resistant to at least RIF and isoniazid (INH) or only RIF; ii) pre-extensively drug-resistant TB (pre-XDR-TB), defined as MDR-TB plus additional resistance to any fluoroquinolone; and iii) extensively drug-resistant TB (XDR-TB), now reclassified as MDR-TB plus additional resistance to any fluoroquinolone and at least one more group A drug.[5,8] Drugs commonly used in the treatment of DR-TB include levofloxacin, bedaquiline, linezolid, clofazimine, delamanid, and amikacin. Many of these drugs are highly toxic and require a long period of treatment, which can exceed 18 months for longer MDR-TB regimens. This immense challenge highlights the need to continuously develop new therapeutic alternatives against DR-TB to achieve the 'End TB Strategy' goals.[3,9]

Although the global scenario sounds alarming, several advances have been achieved in the development of new drugs against DR-TB. In recent years, regulatory agencies around the world have approved three new drugs after decades of inactivity in the discovery and development of new drugs against TB. Delamanid (**1**) and pretomanid (**2**) (Figure 1) were approved in 2014 and 2019, respectively.[10,11] These drugs are representative of the nitroimidazole class. Both are prodrugs that are activated by a deazaflavin-dependent nitroreductase (Ddn), primarily leading to the inhibition of mycolic acid

[a] Dr. G. F. S. Fernandes,[+] K. F. Manieri,[+] A. F. Bonjorno, Dr. D. L. Campos, Dr. C. M. Ribeiro, F. M. Demarqui, Prof. F. R. Pavan, Prof. J. L. Dos Santos
School of Pharmaceutical Sciences
São Paulo State University
Rod. Araraquara-Jaú, Araraquara 14800903 (Brazil)
E-mail: jean.santos@unesp.br
    fernando.pavan@unesp.br
    guilhermefelipe@outlook.com

[b] Dr. G. F. S. Fernandes,[+] Prof. W. A. Denny, Dr. A. M. Thompson
Auckland Cancer Society Research Centre
Faculty of Medical and Health Sciences
The University of Auckland
Private Bag 92019, Auckland 1142 (New Zealand)
E-mail: am.thompson@auckland.ac.nz

[c] D. A. G. Ruiz, Prof. N. M. Nascimento-Junior
Institute of Chemistry, São Paulo State University
Rua Professor Francisco Degni, 55, Araraquara 14800060 (Brazil)

[d] Dr. G. F. S. Fernandes[+]
Present address:
Department of Chemistry, University College London
20 Gordon Street, London WC1H 0AJ, (UK)

[+] These authors contributed equally to this work.

Supporting information for this article is available on the WWW under https://doi.org/10.1002/cmdc.202300015

ChemMedChem

Research Article
doi.org/10.1002/cmdc.202300015

Chemistry Europe
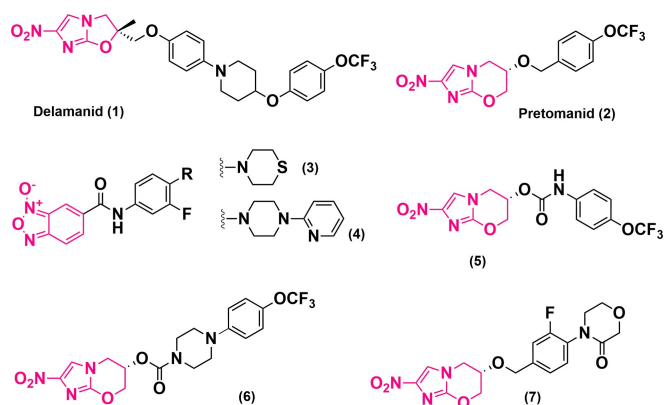European Chemical
Societies Publishing

Figure 1. Two recently approved drugs for MDR-TB, lead benzofuroxan derivatives, and imidazo[2,1-*b*][1,3]oxazine derivatives.

biosynthesis.[12,13] However, an additional mode of action has been reported, which involves the generation of reactive nitrogen species, including nitric oxide, which interferes with cellular respiration.[14–16] Delamanid (**1**) was previously recommended by the WHO for use in longer MDR-TB treatment regimens.[17] Recently, the WHO released some updated guidelines for the treatment of DR-TB. Their report recommends implementing a new drug combination to treat almost all forms of DR-TB. The new recommendation includes BPaLM (a combination of bedaquiline, pretomanid, linezolid, and moxifloxacin) or BPaL (bedaquiline, pretomanid, and linezolid).[18] Despite the recent and significant advances these new drugs bring to the treatment outcomes of DR-TB, resistant strains of *Mtb* have already been identified,[19–21] highlighting the importance of the discovery and development of new compounds.

Recently, our research group identified highly selective benzofuroxan derivatives with potent activity against MDR-TB strains and *in vivo* sterilizing antitubercular activity.[22,23] Compounds **3** and **4** (Figure 1) showed highly promising results, with MIC$_{90}$ values below 0.5 µM against several MDR strains of clinical isolates of *Mtb*. These analogues present the benzofuroxan moiety in their structure, which was shown to be critical for the potent anti-*Mtb* activity since its replacement with other heterocyclics led to a considerable loss of activity.[23]

Therefore, in a continuing effort to develop new anti-TB molecules, we sought another heterocyclic system that could replace benzofuroxan. We selected the imidazo[2,1-*b*][1,3]oxazine moiety for this endeavour, which proved to be a highly beneficial choice. The 2-nitro-6,7-dihydro-5*H*-imidazo[2,1-*b*][1,3]oxazine subunit is the pharmacophore group in the antitubercular drug pretomanid (**2**) and is a close analogue of the 6-nitro-2,3-dihydroimidazo[2,1-*b*][1,3]oxazole moiety present in delamanid (**1**). There is an immense amount of accumulated evidence related to the imidazo[2,1-*b*][1,3]oxazine scaffold that places it in a prominent position in TB drug discovery.[24] Furthermore, a large number of imidazo[2,1-*b*][1,3]oxazine derivatives with potent and promising anti-TB activity have already been reported.[24–30]

The drug design rationale behind the new series was based on previously reported studies of imidazo[2,1-*b*][1,3]oxazines. For example, Blaser *et al.*[31] showed that changing the linker group from OCH$_2$ (**2**) to *O*-carbamate (**5**) (Figure 1) improved the *in vitro* potency by 4 times. Furthermore, when they switched to the arylpiperazine carbamate (**6**) (Figure 1), potency and solubility improved further compared to **5**.[31] In another study, Rakesh *et al.*[32] reported a series of pretomanid-oxazolidinone hybrids as anti-TB agents. The introduction of a 3-fluorophenyl attached to a cyclic amine (**7**) (Figure 1) was shown to lead to improved physicochemical properties compared to pretomanid (**2**).[32] However, unlike **6**, none of the compounds tested in this latter series exhibited any significant efficacy in the chronic mouse model of *Mtb* infection.[32] Taking into account these data, the new series presented here was designed to incorporate the 2-nitro-6,7-dihydro-5*H*-imidazo[2,1-*b*][1,3]oxazine "warhead", *O*-carbamate as a linker, and the best 3-fluorophenyl side chains identified in our previous study.[23]

This strategy led us to the identification of a new and more potent series of imidazo[2,1-*b*][1,3]oxazine derivatives against MDR-TB. Additionally, most of the compounds were also capable of inhibiting intramacrophage mycobacterial growth and were not toxic in the different models evaluated.

Results and Discussion

Chemistry

First, the key intermediate (6*S*)-2-nitro-6,7-dihydro-5*H*-imidazo[2,1-*b*][1,3]oxazin-6-ol (**15**) (Scheme 1) was synthesized according to the methods described previously.[33–35] Briefly, the synthesis started with protection of the (*R*)-glycidol hydroxyl group (**8**) as a triisopropylsilyl (TIPS) ether. The intermediate obtained (**9**) was then reacted with 2-chloro-4-nitro-1*H*-imidazole (**10**), leading to the formation of compound **11** in a regioselective manner. The hydroxyl group of intermediate **11** was then protected as a tetrahydropyranyl (THP) ether (**12**). Subsequently, the TIPS protecting group was removed using tetrabutylammonium fluoride (TBAF), and the alcohol product
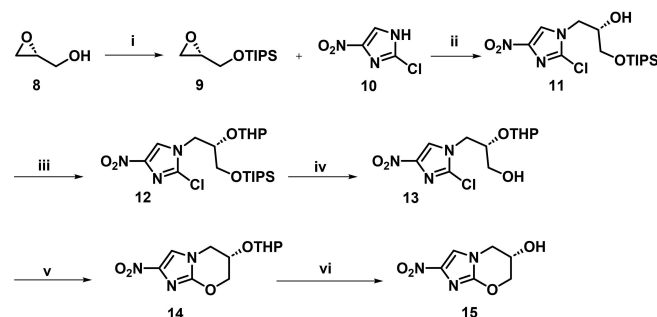
Scheme 1. Synthetic route for the preparation of imidazo[2,1-*b*][1,3]oxazine intermediate **15**. Reagents and conditions: (i) TIPSCl, imidazole, DMAP, DCM, 0–20°C, 12 h, 70%; (ii) DIPEA, toluene, 70°C, 36 h, 86%; (iii) DHP, PPTS, DCM, 20°C, 48 h, 94%; (iv) TBAF, THF, 20°C, 1 h, 89%; (v) NaH 60%, DMF, 0–20°C, 6 h, 37%; (vi) HCl, MeOH, 0–20°C, 20 h, 92%.

ChemMedChem

Research Article
doi.org/10.1002/cmdc.202300015

**Chemistry
Europe**
European Chemical
Societies Publishing

was ring closed with sodium hydride, giving **14**. Finally, the THP group was removed using hydrochloric acid, to give the imidazo[2,1-*b*][1,3]oxazine intermediate **15** (Scheme 1).

Second, a series of aromatic amino intermediates was synthesized following previously reported methodologies.[23,36,37] Initially, nitroaromatic intermediates **27–36** (Scheme 2) were obtained by reacting 3,4-difluoronitrobenzene (**26**) with the appropriate cyclic amine (**16-25**). Then, the required aromatic amino intermediates **37–46** were obtained by catalytic hydrogenation using palladium/carbon.

Lastly, the imidazo[2,1-*b*][1,3]oxazine intermediate **15** was coupled with 1.1 equivalents of the appropriate amines (**37–46**) to generate the final carbamate products (**47-56**). This reaction was accomplished using 0.5 equivalents of triphosgene as the carbonyl source in tetrahydrofuran (THF) (Scheme 3).[31]

In vitro antimycobacterial activity and cytotoxicity evaluation

Initially, the library of imidazo[2,1-*b*][1,3]oxazine derivatives (**47-56**) was screened *in vitro* against *Mtb* H37Rv (ATCC 27294) using the Resazurin Microtiter Assay (REMA) method.[38] The results were recorded as the Minimum Inhibitory Concentration that inhibited 90% of bacterial growth (MIC_{90}). In general, the
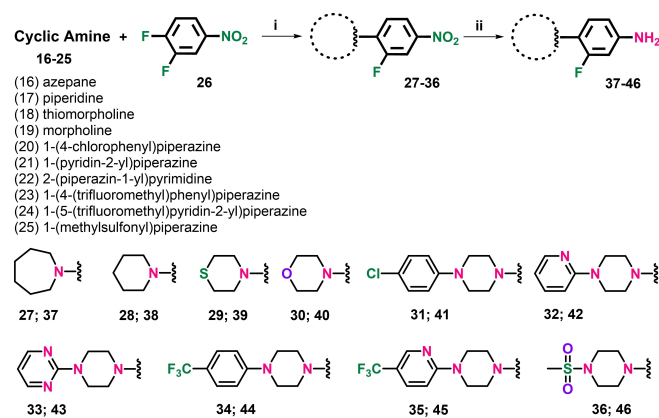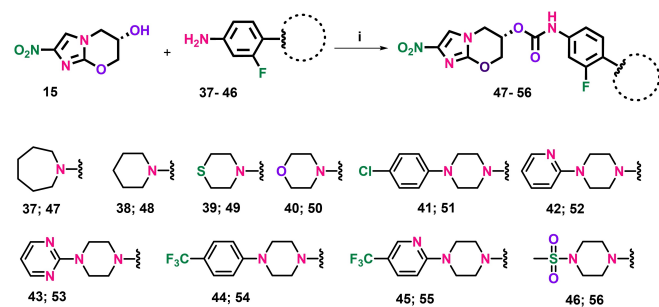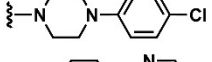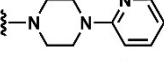
compounds tested showed excellent antimycobacterial activity, with MIC_{90} values ranging from 0.18 to 1.63 µM (Table 1). Nine of the ten final compounds evaluated exhibited MIC_{90} values below 0.35 µM, implying activity superior to that of **7** (MIC 1.99 µM),[32] and broadly comparable to that of **5** (MIC_{90} 0.12 µM).[31]

The essential difference between the imidazo[2,1-*b*][1,3]oxazine derivatives presented here and previously reported benzofuroxans,[22] is the replacement of the benzofuroxan nucleus with the 2-nitro-6,7-dihydro-5*H*-imidazo[2,1-*b*][1,3]oxazine moiety. Furthermore, we exchanged the amide with carbamate[39] as a linker between the imidazo[2,1-*b*][1,3]oxazine core and the side chain. The choice of the substitution pattern in the side chain rings was based on the results observed previously for the benzofuroxan derivatives.[23] Substituents that presented the best activity profile in the previous series were used here. In addition, we included new substituents, such as trifluoromethyl (**54**, **55**) and methylsulphonyl (**56**), to expand the analysis and understanding of the importance of different groups for biological activity. All compounds except **56** exhibited potent effects against *Mtb*, making it difficult to determine a structure-activity relationship (SAR) for this series. Nevertheless, it is evident that incorporation of the 2-nitro-6,7-dihydro-5*H*-imidazo[2,1-*b*][1,3]oxazine moiety significantly improved activity since analogous benzofuroxan derivatives[23] did not have such potent MIC_{90} values.

The imidazo[2,1-*b*][1,3]oxazine derivative **56**, containing a sulphonamide in the structure, was the only analogue with a MIC_{90} value greater than 1 µM (1.63 µM). The less potent activity of **56** may be related to the physicochemical properties of the molecule. Compound **56** had the lowest cLogD value (1.51) within the series. All other compounds displayed cLogD values greater than 2.7 and were more potent than compound **56**. These data suggest the influence that physiochemical properties, especially logD, exert on the activity of this series. Intriguingly, several other sulphonamide-containing pretomanid derivatives were previously reported to have inferior activity, implying a poor tolerance for this group across the imidazo[2,1-*b*][1,3]oxazine class.[28,31] Although **56** has a higher MIC compared to the other analogues, it still has significant activity, being more potent than several anti-TB compounds currently in preclinical studies.[5]

Despite the difficulty in establishing an SAR relationship, we can observe some patterns. For instance, compounds **54** and **55**, with MIC_{90} values of 0.18 µM, are very similar and the only difference between them is the substitution of the phenyl ring (**54**) for a pyridine ring (**55**). Additionally, both analogues contain a trifluoromethyl substituent in the structure, suggesting the importance of this group for antimycobacterial activity. Compounds **48**, **49**, and **50** also display similar structures, with the only difference being the cyclic ring attached to the fluorophenyl ring. It is evident here that compounds with higher cLogD values demonstrated more potent activity. For example, compounds **48** and **49**, which bear a piperidine and a thiomorpholine ring, respectively, were more active than the morpholine analogue (**50**). Compound **50** has a cLogD of 2.72 while compounds **48** and **49** have higher cLogD values, 3.79

Scheme 2. General synthetic route for the preparation of aromatic amino intermediates **37–46**. Reagents and conditions: (i) DIPEA, acetonitrile, 80 °C, 6 h; (ii) Pd/C, H₂, methanol, 24 h.

Scheme 3. Synthetic route for the preparation of carbamate final compounds **47–56**. Reagents and conditions: (i) triphosgene, triethylamine, THF, 20 °C, 16 h.
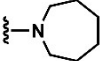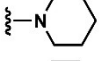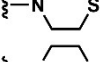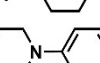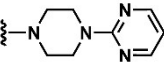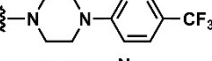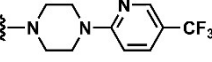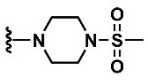
Table 1. *In vitro* activity against *Mtb* H37Rv (MIC$_{90}$), cytotoxicity (IC$_{50}$), selectivity index (SI), and clogD values of imidazo[2,1-*b*][1,3]oxazine derivatives **47–56**.

Compd	R	MIC$_{90}$ [μM] H37Rv	HepG2, (SI)[b]	IC$_{50}$ [μM][a] MRC-5, (SI)[b]	J774A-1, (SI)[b]	clogD[c]
47	(azepane) —N	0.34 ± 0.18	477 ± 0, (1403)	270 ± 97, (794)	142 ± 2, (416)	4.23
48	(piperidine) —N	0.24 ± 0.00	459 ± 20, (1911)	179 ± 126, (746)	119 ± 15, (495)	3.79
49	(thiomorpholine) —N S	0.23 ± 0.00	472 ± 0, (2054)	288 ± 162, (1252)	143 ± 12, (621)	3.30
50	(morpholine) —N O	0.32 ± 0.09	442 ± 43, (1380)	148 ± 29, (463)	142 ± 27, (445)	2.72
51	—N N—(C6H4)—Cl	0.19 ± 0.00	387 ± 0, (2036)	247 ± 138, (1300)	119 ± 5, (626)	5.28
52	—N N—(pyridyl)	0.20 ± 0.00	413 ± 1, (2065)	313 ± 152, (1565)	129 ± 6, (644)	4.01
53	—N N—(pyrimidyl)	0.20 ± 0.00	413 ± 0, (2065)	279 ± 143, (1395)	124 ± 8, (620)	3.43
54	—N N—(C6H4)—CF3	0.18 ± 0.00	323 ± 18, (1794)	176 ± 153, (978)	107 ± 7, (592)	5.55
55	—N N—(pyridyl)—CF3	0.18 ± 0.00	348 ± 26, (1932)	182 ± 127, (1011)	117 ± 3, (648)	4.93
56	—N N—SO2—CH3	1.63 ± 0.04	385 ± 48, (236)	170 ± 102, (104)	127 ± 5, (78)	1.51
BZF **3**[23]		0.70 ± 0.26		57.1 (81)		1.95
BZF **4**[23]		0.09 ± 0.04		>180 (>2085)		2.80
RIF[d]		0.12 ± 0.00				
INH[d]		2.20 ± 0.73				
AMK[d]		0.47 ± 0.14				
MOX[d]		1.11 ± 0.65				

[a] 50% inhibitory concentration (IC$_{50}$) in HepG2 (liver), MRC-5 (lung), and J774 A-1 (murine macrophage) cell lines. [b] Selectivity Index (SI; given by the ratio between IC$_{50}$ and MIC$_{90}$). [c] clogD (pH 7.4) calculated using MarvinSketch, Chemaxon. [d] RIF, rifampicin; INH, isoniazid; AMK, amikacin; MOX, moxifloxacin.

and 3.30, respectively. It is worth noting that the cLogD values were calculated at pH 7.4.

Cytotoxicity studies were carried out in three different cell lines: HepG2 (ATCC HB-8065; liver), MRC-5 (ATCC CCL-171; lung), and J774A-1 (ATCC TIB-67; murine macrophage) according to previously reported procedures.[40,41] The results were expressed as inhibitory concentrations (IC$_{50}$), and the selectivity indices (SI) were calculated as the ratio between the IC$_{50}$ and MIC$_{90}$ values. Importantly, none of the imidazo[2,1-*b*][1,3]oxazine derivatives showed cytotoxicity in the cell lines evaluated. The IC$_{50}$ values for all the analogues were greater than 322 μM in HepG2, 147 μM in MRC-5, and 106 μM in J774A-1, translating into high SI values for all compounds tested.

In vitro determination of activity against intramacrophage Mtb

During active infection and also in the dormant state, *Mtb* lodges mainly inside macrophages.[42,43] Therefore, compounds developed against TB must be able to cross not only the thick lipid wall of *Mtb* but also the cell membrane of macrophages to reach the main reservoir of mycobacteria. Evaluation of intramacrophage activity against *Mtb* is of significant importance in the initial stages of the development of new anti-TB drugs.[44]

Here, we assessed the intramacrophage activity of the compounds in J774A.1, a mouse macrophage cell line, and the results are shown in Figure 2. All compounds were tested at their MIC$_{90}$ concentrations, as previously stipulated in the REMA assay, against *Mtb* H37Rv (ATCC 27294). The analogues showed significant inhibition of intracellular bacterial growth in a dose-dependent manner compared to controls. For example, several
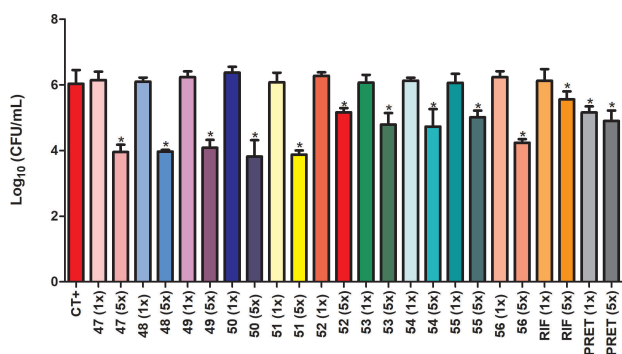
ChemMedChem

Research Article
doi.org/10.1002/cmdc.202300015

Chemistry Europe
European Chemical
Societies Publishing

Figure 2. Intramacrophage activity of new analogues, rifampicin, and pretomanid, after infection of J774A.1 macrophages with *Mtb* H37Rv (ATCC 27294).

compounds, including **47** and **51**, showed a 2-log reduction in bacterial burden compared to the positive control.

Furthermore, these compounds were able to inhibit bacterial growth much more effectively than the drugs used as controls, rifampicin and pretomanid. Although these drugs are currently used in the clinic, the new analogues described herein were superior in inhibiting intramacrophage mycobacterial growth. For example, compounds **47** and **51** reduced the bacterial load by more than 1 log relative to the rifampicin and pretomanid-treated infected macrophages.

Further *in vitro* activity against Mtb drug-resistant strains

The emergence of DR strains is the main concern of health authorities around the world. Currently, drug discovery campaigns aim to discover potential drugs against resistant forms of TB (MDR- and XDR-TB).[5] Consequently, we tested all of the compounds described here against a panel of clinical isolates (CI). These strains were phenotypically characterized and exhibited resistance to several anti-TB drugs.[45] Specifically, each CI strain exhibited resistance to at least the following

drugs: CI-3: RIF; CI-4: INH and RIF; CI-5: INH and RIF; CI-6: INH and RIF; CI-7: INH and RIF. CI-1 and CI-2 were characterized as susceptible strains. The strains were classified as MDR based on the MIC_{90} values of the control drugs against them.

Table 2 shows the results of the *in vitro* evaluation against this panel of clinical isolates. The concentration for the determination of promising compounds versus resistant strains was defined as 5 μM. Overall, all the compounds tested exhibited potent activity against most of the clinical isolates assayed. For instance, the most promising compounds, **47**, **48**, **49**, **51**, **52**, **53** and **55** displayed MIC_{90} values below 0.5 μM against most clinical isolates, including MDR strains. As noted for the susceptible strain (H37Rv), the characterization of an SAR is a challenge, and it is not possible to establish a clear relationship between the antimycobacterial activity and the chemical structure of these compounds.

In vitro determination of activity against Gram-positive and negative bacteria and *Candida albicans*

Treatment of TB requires a long period. Hence, it is essential that the drugs used are highly selective against *Mtb*. Therefore, we tested the analogues against a panel of Gram-positive and negative bacteria and *Candida albicans*. Table 3 shows the results against 4 different bacterial species, namely *Escherichia coli* (ATCC 25922), *Staphylococcus aureus* (ATCC 25923), *Salmonella typhi* (ATCC 14028) and *Pseudomonas aeruginosa* (ATCC 27853), as well as the results against a fungus commonly found in the human microbiota, *Candida albicans* (ATCC 90028). As shown in Table 3, none of the compounds showed significant antibacterial or antifungal activity against the evaluated strains.

In vivo evaluation of acute toxicity in *Galleria mellonella*

After the initial screening, we decided to proceed with evaluation of the toxicity of the compounds in an *in vivo* model to ensure the safety of the compounds for future preclinical

Table 2. *In vitro* activity against clinical isolates of *Mtb*.							
Compd				MIC_{90} [μM]			
	CI-1[b]	CI-2[b]	CI-3[b]	CI-4[b]	CI-5[b]	CI-6[b]	CI-7[b]
47	1.59 ± 1.92	0.23 ± 0.00	0.43 ± 0.28	0.23 ± 0.00	1.40 ± 0.16	0.23 ± 0.00	0.23 ± 0.00
48	0.32 ± 0.09	0.24 ± 0.00	0.17 ± 0.10	0.24 ± 0.00	5.57 ± 0.93	0.24 ± 0.00	1.50 ± 1.78
49	0.23 ± 0.00	0.33 ± 0.18	0.23 ± 0.00	0.23 ± 0.00	0.77 ± 0.05	0.23 ± 0.00	5.36 ± 7.25
50	0.24 ± 0.00	0.58 ± 0.59	0.45 ± 0.01	0.31 ± 0.10	3.22 ± 0.19	0.62 ± 0.33	3.08 ± 3.15
51	0.19 ± 0.00	0.19 ± 0.00	0.19 ± 0.00	0.19 ± 0.00	0.19 ± 0.00	0.19 ± 0.00	4.46 ± 6.04
52	0.20 ± 0.00	0.20 ± 0.00	0.20 ± 0.00	0.20 ± 0.00	1.18 ± 0.12	0.20 ± 0.00	7.99 ± 11.02
53	0.20 ± 0.00	0.30 ± 0.17	0.20 ± 0.00	0.20 ± 0.00	21.5 ± 0.4	0.42 ± 0.39	0.20 ± 0.00
54	0.18 ± 0.00	0.38 ± 0.34	0.39 ± 0.29	0.18 ± 0.00	43.1 ± 3.3	0.18 ± 0.00	44.6 ± 1.2
55	0.18 ± 0.00	0.18 ± 0.00	0.18 ± 0.00	0.18 ± 0.00	16.0 ± 3.0	0.62 ± 0.52	1.20 ± 1.44
56	1.36 ± 0.27	1.03 ± 0.59	3.32 ± 1.39	1.08 ± 0.42	6.32 ± 0.17	2.02 ± 1.87	3.97 ± 1.76
RIF[a]	0.13 ± 0.01	0.12 ± 0.00	0.12 ± 0.00	15.3 ± 21.4	0.12 ± 0.00	0.71 ± 1.02	30.4 ± 0.0
INH[a]	11.1 ± 0.1	28.6 ± 30.1	182 ± 0	31.6 ± 0.0	ND	2.24 ± 0.00	30.4 ± 0.0
MOX[a]	0.27 ± 0.00	0.97 ± 0.37	1.03 ± 0.51	1.53 ± 0.00	ND	1.02 ± 1.10	ND
PRET[a]	ND	0.80 ± 0.92	0.27 ± 0.00	ND	ND	ND	ND
[a] INH: isoniazid; RIF: rifampicin; MOX: moxifloxacin; PRET: pretomanid; ND: not determined; recorded data are the average of the results from two or three independent assays. [b] CI: clinical isolate; CI-1: sensitive strain; CI-2: sensitive strain; CI-3: RIF-resistant strain; CI-4 - 7: MDR strains.							

ChemMedChem

Research Article
doi.org/10.1002/cmdc.202300015

Chemistry Europe
European Chemical
Societies Publishing

Table 3. *In vitro* spectrum of activity of the compounds.

Compd	MIC$_{90}$ [µM]				
	Escherichia coli (ATCC 25922)	*Staphylococcus aureus* (ATCC 25923)	*Salmonella typhi* (ATCC 14028)	*Pseudomonas aeruginosa* (ATCC 27853)	*Candida albicans* (ATCC 90028)
47	59.6	59.6	59.6	59.6	179
48	61.7	61.7	61.7	61.7	247
49	59.1	59.1	59.1	44.3	236
50	61.4	61.4	61.4	38.4	138
51	48.4	48.4	48.4	48.4	48.4
52	51.7	38.8	51.7	29.1	207
53	51.6	51.6	51.6	27.4	206
54	45.4	45.4	45.4	25.6	22.7
55	45.3	45.3	45.3	45.3	181
56	51.6	51.6	51.6	29.0	206
Gentamicin	1.90	0.63	0.95	0.47	–
Amphotericin B	–	–	–	–	1.45

evaluation. We selected *Galleria mellonella* larvae as a model for the acute toxicity test.[46] Compounds **47** and **49** were selected for this assay because they showed the best solubility profile in the lipid-soluble vehicles used in the assay. For the assay, compound **47** was solubilized at the ideal concentration of 2,000 mg/kg of mean body weight of the larvae group, while compound **49** was only able to be solubilized at half of this concentration (1,000 mg/kg of body weight). The evaluated compounds did not show any toxicity to the larvae at the concentrations tested (Figure 3).

Molecular docking studies and *in silico* prediction of ADME properties

To comprehend the poses and interactions of the synthesized compounds (**47**-**56**) and the activating deazaflavin-dependent nitroreductase holoenzyme (h-Ddn) of *Mtb*, an *in silico* model was built, starting with the 3D structure of full-length h-Ddn generated from the AlphaFold web server (Supplementary Material: Figure S63).[47] The docking calculations were based on the modelled h-Ddn structure and the parent drug pretomanid.
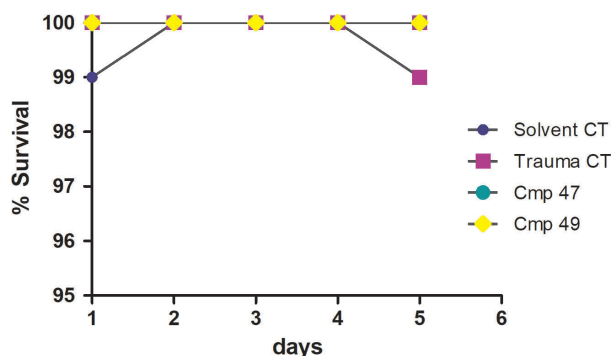
Validation of the study was carried out by observing interactions involving the key amino acid residues F17, S78, and Y133, and the 2-nitro-6,7-dihydro-5*H*-imidazo[2,1-*b*][1,3]oxazine moiety in its suggested orientation, according to the literature.[48–51] Compared to pretomanid, all synthesized compounds (**47**–**56**) (Figure 4) showed similar interactions in the catalytic pocket of h-Ddn. Most of the compounds interact through hydrogen bonds involving the Y133 and S78 residues, at distances ranging from 2.1 Å (compound **56**) to 2.7 Å (compound **55**) and from 1.5 Å (compound **54**) to 2.1 Å (compound **55**), respectively.

Herein, we found that the Y133 residue plays a key role in the catalytic activity of the enzyme by also forming a hydrogen bond with the required cofactor F420, as reported.[48,50] Specifically, we observed a bifurcated hydrogen bond[52] between the hydroxyl group of Y133, the C4 carbonyl oxygen of the F420 isoalloxazine moiety, and the nitro group of the imidazo[2,1-*b*][1,3]oxazine scaffold, which helps to anchor these two ring systems. Interestingly, the latter binding pattern (involving Y133 and the nitro group of pretomanid) was not identified in a previous molecular dynamics study based on a reconstructed homology model of full-length h-Ddn.[50] Additionally, our results revealed that the Y130 amino acid residue does not

Figure 3. Percentage survival of *G. mellonella* larvae in 5 days of treatment at a concentration of 2,000 mg/kg for **47** and 1,000 mg/kg for **49**. Solvent CT – group of larvae that received only the vehicle for the compounds studied to evaluate a possible toxicity reaction by the solvent substance; CT Trauma – group of larvae that received the application of 1x PBS solution, so that the trauma caused by the needle was evaluated as a possible cause of death.

Figure 4. Interacting residues of h-Ddn and score values for **47**–**56** and pretomanid. [a]PRET: Pretomanid interactions with Ddn residues according to the docking validation method.

ChemMedChem

Research Article
doi.org/10.1002/cmdc.202300015

Chemistry Europe
European Chemical
Societies Publishing

interact with the ligand, contrary to the proposal made by Cellitti *et al.* (2012) (these authors modelled the nitroimidazooxazine core of pretomanid into a cocrystal structure of F420 bound to a truncated Ddn construct lacking 40 residues from the N-terminus).[48] Here, the afore-mentioned molecular dynamics studies conducted by Mohamed *et al.* (2016) support our finding, indicating that the role of the Y130 residue is to act as part of a hydrophobic barrier (together with Y65 and Y136) in the active site of Ddn.[50] Like the latter authors, we also observed π–π stacking interactions with cofactor F420 (cF420) for all compounds. This is in line with an activation mechanism that involves hydride transfer from C5 of the deprotonated cofactor to the C3 atom of the imidazo[2,1-*b*][1,3]oxazine substrate (ultimately leading to the release of reactive nitrogen species).[50] Furthermore, the tail portion of all compounds studied showed intermolecular interactions with the α-helix of h-Ddn, particularly π-alkyl and/or π–π stacking interactions involving the residues F17 and W20, as well as sulfur-π or π-alkyl interactions with M21, involving the side chain phenyl group. The best scores in Figure 4 affirm that interactions with aromatic residues belonging to the α-helix of h-Ddn are important for the activity, as mentioned by Cellitti *et al.* (2012), especially the interaction with W20.[48]

Analysis of the docking results revealed that intermolecular interactions involving h-Ddn and the ligands **47**, **49** and pretomanid occurred through the same amino acid residues. The key amino acid residues Y133 and S78 interact with the mentioned ligands through hydrogen bond interactions with the nitro group of the imidazo[2,1-*b*][1,3]oxazine moiety, as shown in Figure 5. Additionally, **47** forms a halogen bond
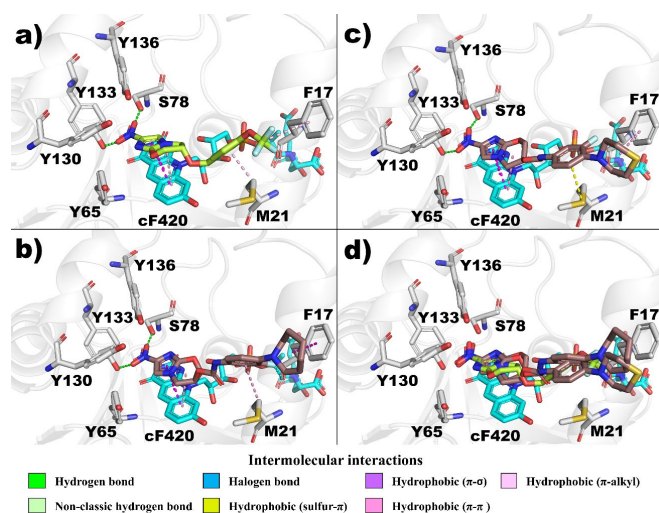
between the fluorine atom in the aromatic subunit and the carbonyl group located in the backbone of F17 (Figure 5b). On the other hand, in Figure 5d, it was possible to identify the similar orientation of ligands **47** and **49**; therefore, their similar biological activity could be explained by their interaction with the same regions of h-Ddn (catalytic pocket with hydrogen bond donor residues, cofactor F420 with π-alkyl and π–π stacking interactions and α-helix with aromatic hydrophobic residues). Although pretomanid also has the same orientation and interactions, rotatable covalent bonds at the final part of the pretomanid tail could allow additional interaction with complementary amino acid residues, such as F16 and W20.[48,50] Therefore, the conformational restrictions arising from terminal heterocyclic moieties in the tail of compounds **47** and **49** restrict the required torsion for interactions involving the F16 and W20 residues from the α-helix of h-Ddn.

In silico predictions of ADME properties were obtained by Swiss ADME software (Supplementary material). Compounds **47–56** were mostly soluble or moderately water-soluble and all have the potential to be absorbed after oral administration (> 82.6%). The data suggest that compounds **47–56** are not substrates for CYP3A4, CYP2D6, and CYP1A2; however, all seem to be substrates for CYP2C19. *In silico* data also suggest that compounds **47–56** are not hERG inhibitors. Finally, compounds **47–49** did not violate any parameter of Lipinski's rules.

Conclusions

Herein, we present the continuation of our medicinal chemistry campaign that aimed to develop new anti-TB compounds. We designed and synthesized a series of new imidazo[2,1-*b*][1,3]oxazine derivatives through a lead optimization strategy based on benzofuroxan derivatives previously identified in our research group. The selection of the 2-nitro-6,7-dihydro-5*H*-imidazo[2,1-*b*][1,3]oxazine subunit to replace benzofuroxan was motivated by the fact that it is the pharmacophoric group of the anti-TB drug pretomanid and compounds containing this scaffold often exhibit high selectivity and potency against *Mtb*. Furthermore, we have included the *O*-carbamate group as a linker and a series of different side chains containing the 3-fluorophenyl attached to a cyclic amine. In total, we synthesized and characterized ten new imidazo[2,1-*b*][1,3]oxazine derivatives. We tested these compounds in a series of experiments designed to assess their potential as anti-TB agents, including evaluation against susceptible strains and MDR clinical isolates of *Mtb*, selectivity against a panel of different microorganisms, activity against intramacrophage *Mtb*, and toxicity toward *in vitro* and *in vivo* models. The new series of imidazo[2,1-*b*][1,3]oxazine derivatives showed high potencies against *Mtb* H37Rv, with MIC_{90} values ranging from 0.18 to 1.63 μM. Additionally, most of the compounds displayed MIC_{90} values below 0.5 μM against a panel of MDR clinical isolates. Finally, the compounds did not show toxicity toward *in vitro* or *in vivo* models and showed potent intramacrophage activity. Molecular modelling studies suggest that all compounds interact with the deazaflavin-dependent nitroreductase holoenzyme in poses

Figure 5. Analysis of the docking poses for compounds **47** and **49**, compared to pretomanid. First docking pose and interactions with h-Ddn of a) pretomanid (PA-824), b) compound **47**, c) compound **49**, d) superposition of compounds **47**, **49** and pretomanid, involving the catalytic pocket. All hydrogen atoms were omitted for clarity. Carbon atoms are shown in brown (for **47** and **49**), in light green (for pretomanid), in cyan (for cF420), and in white (for Ddn). In addition, fluorine atoms are shown in light cyan, oxygen atoms in red, nitrogen atoms in blue, phosphorus atoms in orange, and sulfur atoms in yellow for all structures. The intermolecular interactions are indicated as dotted lines.

ChemMedChem

Research Article
doi.org/10.1002/cmdc.202300015

Chemistry Europe
European Chemical
Societies Publishing

similar to those found for pretomanid. The results presented here demonstrate the potential of this new series of compounds. The compounds showed potent activity against several MDR strains of *Mtb* and thus will advance to the next stages of development in due course.

Experimental Section

Chemistry

All reagents, chemicals, and solvents were purchased from commercial suppliers and used without further purification. Reactions were monitored by thin-layer chromatography (TLC) using commercially available precoated plates and visualized with UV light at 254 nm. Flash column chromatography was carried out using Sigma Aldrich silica gel (pore size 60 Å, particle size 35–75 μm). The ^{1}H NMR and ^{13}C NMR spectra were obtained with a Bruker® Avance 400 MHz spectrometer at room temperature (rt) using deuterated chloroform (CDCl$_3$) or dimethylsulfoxide (DMSO-d$_6$) as solvents. Chemical shifts were expressed in parts-per-million (ppm) relative to tetramethylsilane (TMS). The coupling constants (*J*) are denoted in hertz (Hz). Spin multiplicities were reported as singlet (s), doublet (d), triplet (t), quartet (q), multiplet (m), doublet of doublet (dd) and doublet of doublet of doublets (ddd). HPLC purity analysis for the final compounds confirmed that they were greater than 95%. HPLC analysis was carried out using a Shimadzu® HPLC model CBM20-A coupled with a UV-VIS detector (model SPD-20 A) and an Agilent® Eclipse XDB C-18 column (250 mm ×274.6 mm; 5 μm). HPLC method A: methanol-water 70:30. Melting points (mp) were recorded with an electrothermal melting point apparatus Mettler FP82+FP80 (Greifense, Switzerland). LC–MS measurements were recorded on a Thermo Fisher Scientific Finnigan Surveyor MSQ single-quadrupole mass spectrometer. Compounds **15**, **37**, **39**, **40**, **41**, **42**, and **43** were synthesized according to the methodologies described previously. Experimental details for the synthesis and characterization of all prepared compounds are provided in the Supporting Information. The characterization data for the final compounds are presented below.

General method for carbamate synthesis (47–56)

Compound **15** (26 mg, 0.144 mmol) was suspended in 3 mL of dry THF (3 mL) under N$_2$ (sealed after degassing) and treated with Et$_3$N (90 μl, 0.575 mmol), then cooled on ice. Triphosgene (51 mg, 0.173 mmol) was added, and the mixture was sealed under N$_2$ and stirred at 20 °C for 2 h (a white suspension was formed). A solution of the appropriate amine (**37–46**) (0.144 mmol) in dry THF (1 mL) was added using a syringe and the resulting mixture was stirred at 20 °C for 14 h. The reaction mixture was quenched with aqueous NaHCO$_3$, then water was added, and the mixture was extracted with CH$_2$Cl$_2$. The combined extracts were dried over Na$_2$SO$_4$ and then evaporated under reduced pressure. The crude product was purified by flash chromatography using EtOAc:hexane (90:10, v/v) as the mobile phase to give the final carbamates (**47-56**) as off-white solids in varying yields.

(*S*)-2-Nitro-6,7-dihydro-5*H*-imidazo[2,1-*b*][1,3]oxazin-6-yl (4-(azepan-1-yl)-3-fluorophenyl)carbamate (47)

Off-white solid; yield 24%; mp: 198–201 °C; R$_f$=0.46 (EtOAc-*n*-hexane, 9:1). ^{1}H NMR (400 MHz, DMSO-d$_6$) δ: 9.76 (s, 1H, NH$_{carbamate}$), 8.08 (s, 1H, CH$_{aromatic}$), 7.24 (d, *J*=15.6 Hz, 1H, CH$_{aromatic}$), 7.04 (d, *J*=8.4 Hz, 1H, CH$_{aromatic}$), 6.85 (t, *J*=9.6 Hz, 1H, CH$_{aromatic}$), 5.41–5.37 (m,

1H, CH$_{oxazine}$), 4.64–4.61 (m, 2H, CH$_{2oxazine}$), 4.46–4.37 (m, 1H, CH$_{oxazine}$), 4.34–4.27 (m, 1H, CH$_{oxazine}$), 3.23 (t, *J*=5.5 Hz, 4H, CH$_{2azepane}$), 1.75–1.69 (m, 4H, CH$_{2azepane}$), 1.56–1.52 (m, *J*=2.6 Hz, 4H, CH$_{2azepane}$). ^{13}C NMR (100 MHz, DMSO-d$_6$) δ: 153.6; 152.0; 151.2; 146.8; 135.2 (d, J_{C-F}=8.6 Hz, 1 C); 130.2 (d, J_{C-F}=11.4 Hz, 1 C); 117.9; 117.6 (d, J_{C-F}=4.9 Hz, 1 C); 114.6; 106.9 (d, J_{C-F}=25.8 Hz, 1 C); 68.5; 62.6; 51.7 (2 C); 47.0; 28.4 (2 C); 26.6 (2 C). MS/APCI m/z: calcd for C$_{19}$H$_{22}$FN$_5$O$_5$ 419.2, found: [M+H]$^+$ 420.2.

(*S*)-2-Nitro-6,7-dihydro-5*H*-imidazo[2,1-*b*][1,3]oxazin-6-yl (3-fluoro-4-(piperidin-1-yl)phenyl)carbamate (48)

Off-white solid; yield 41%; mp: 232–235 °C; R$_f$=0.49 (EtOAc-*n*-hexane, 9:1). ^{1}H NMR (400 MHz, DMSO-d6) δ: 9.88 (s, 1H, NH$_{carbamate}$), 8.08 (s, 1H, CH$_{aromatic}$), 7.29 (d, *J*=14.6 Hz, 1H, CH$_{aromatic}$), 7.12 (d, *J*=8.0 Hz, 1H, CH$_{aromatic}$), 6.95 (t, *J*=9.3 Hz, 1H, CH$_{aromatic}$), 5.41 (d, *J*=1.5 Hz, 1H, CH$_{oxazine}$), 4.63 (s, 2H, CH$_{2oxazine}$), 4.41 (dd, *J*=13.9, 3.4 Hz, 1H, CH$_{2oxazine}$), 4.31 (d, *J*=14.0 Hz, 1H, CH$_{2oxazine}$), 2.90–2.84 (m, 4H, CH$_{2piperidine}$), 1.66–1.58 (m, 4H, CH$_{2piperidine}$), 1.50 (dd, *J*=11.1, 5.7 Hz, 2H, CH$_{2piperidine}$). ^{13}C NMR (100 MHz, DMSO-d$_6$) δ: 156.9; 153.5; 152.0; 146.8; 136.2 (d, J_{C-F}=9.0 Hz, 1 C); 133.4 (d, J_{C-F}=10.4 Hz, 1 C); 119.6 (d, J_{C-F}=4.0 Hz, 1 C); 117.9; 114.3; 106.6 (d, J_{C-F}=25.3 Hz, 1 C); 68.5; 62.7; 51.7 (2 C); 47.0; 25.7 (2 C); 23.7. MS/APCI m/z: calcd for C$_{18}$H$_{20}$FN$_5$O$_5$ 405.1, found: [M+H]$^+$ 406.2, [M+Cl]$^-$ 440.2.

(*S*)-2-Nitro-6,7-dihydro-5*H*-imidazo[2,1-*b*][1,3]oxazin-6-yl (3-fluoro-4-thiomorpholinophenyl)carbamate (49)

Off-white solid; yield 22%; mp: 233–236 °C; R$_f$=0.80 (EtOAc-*n*-hexane, 9:1). ^{1}H NMR (400 MHz, DMSO-d6) δ: 9.93 (s, 1H, NH$_{carbamate}$), 8.08 (s, 1H, CH$_{aromatic}$), 7.31 (d, *J*=14.1 Hz, 1H, CH$_{aromatic}$), 7.14 (d, *J*=8.0 Hz, 1H, CH$_{aromatic}$), 7.01 (t, *J*=9.2 Hz, 1H, CH$_{aromatic}$), 5.41 (d, *J*=1.4 Hz, 1H, CH$_{oxazine}$), 4.63 (s, 2H, CH$_{2oxazine}$), 4.41 (dd, *J*=13.9, 3.4 Hz, 1H, CH$_{2oxazine}$), 4.31 (d, *J*=13.9 Hz, 1H, CH$_{2oxazine}$), 3.17–3.13 (m, 4H, CH$_{2thiomorpholine}$), 2.74–2.70 (m, 4H, CH$_{2thiomorpholine}$). ^{13}C NMR (100 MHz, DMSO-d$_6$) δ: 156.0; 153.6; 152.0; 146.8; 135.9 (d, J_{C-F}=9.2 Hz, 1 C); 134.1 (d, J_{C-F}=11.2 Hz, 1 C); 120.8 (d, J_{C-F}=3.6 Hz, 1 C); 117.9; 114.3; 106.5 (d, J_{C-F}=25.8 Hz, 1 C); 68.5; 62.8; 53.1 (2 C); 46.9; 27.2 (2 C). MS/APCI m/z: calcd for C$_{17}$H$_{18}$FN$_5$O$_5$S 423.1, found: [M+H]$^+$ 424.1, [M+Cl]$^-$ 458.0.

(*S*)-2-Nitro-6,7-dihydro-5*H*-imidazo[2,1-*b*][1,3]oxazin-6-yl (3-fluoro-4-morpholinophenyl)carbamate (50)

Off-white solid; yield 30%; mp: 212–215 °C; R$_f$=0.64 (EtOAc-*n*-hexane, 9:1). ^{1}H NMR (400 MHz, DMSO-d6) δ: 9.92 (s, 1H, NH$_{carbamate}$), 8.08 (s, 1H, CH$_{aromatic}$), 7.32 (d, *J*=14.3 Hz, 1H, CH$_{aromatic}$), 7.15 (d, *J*=7.6 Hz, 1H, CH$_{aromatic}$), 6.97 (t, *J*=9.3 Hz, 1H, CH$_{aromatic}$), 5.41 (d, *J*=1.4 Hz, 1H, CH$_{oxazine}$), 4.63 (s, 2H, CH$_{2oxazine}$), 4.41 (dd, *J*=13.9, 3.3 Hz, 1H, CH$_{2oxazine}$), 4.32 (d, *J*=14.2 Hz, 1H, CH$_{2oxazine}$), 3.73–3.69 (m, 4H, CH$_{2morpholine}$), 2.94–2.90 (m, 4H, CH$_{2morpholine}$). ^{13}C NMR (100 MHz, DMSO-d$_6$) δ: 155.8; 153.5 (d, J_{C-F}=9.6 Hz, 1 C); 152.0; 146.8; 134.9 (d, J_{C-F}=8.9 Hz, 1 C); 133.8 (d, J_{C-F}=10.3 Hz, 1 C); 119.3 (d, J_{C-F}=3.7 Hz, 1 C); 117.9; 114.3 (d, J_{C-F}=3.5 Hz, 1 C); 106.7 (d, J_{C-F}=14.7 Hz, 1 C); 68.5; 66.1 (2 C); 62.9; 50.7 (2 C); 46.9. MS/APCI m/z: calcd for C$_{17}$H$_{18}$FN$_5$O$_6$ 407.1, found: [M+H]$^+$ 408.1, [M+Cl]$^-$ 442.1.

(*S*)-2-Nitro-6,7-dihydro-5*H*-imidazo[2,1-*b*][1,3]oxazin-6-yl (4-(4-(4-chlorophenyl)piperazin-1-yl)-3-fluorophenyl)carbamate (51)

Off-white solid; yield 31%; mp: 236–239 °C; R$_f$=0.75 (EtOAc-*n*-hexane, 9:1). ^{1}H NMR (400 MHz, DMSO-d6) δ: 9.94 (s, 1H, NH$_{carbamate}$), 8.09 (s, 1H, CH$_{aromatic}$), 7.34 (d, *J*=14.3 Hz, 2H, CH$_{aromatic}$), 7.03 (t, *J*=

ChemMedChem

Research Article
doi.org/10.1002/cmdc.202300015

**Chemistry
Europe**

European Chemical
Societies Publishing

9.4 Hz, 1H, CH$_{aromatic}$), 6.98 (d, J=7.9 Hz, 2H, CH$_{aromatic}$), 6.80 (t, J=7.3 Hz, 1H, CH$_{aromatic}$), 5.42 (d, J=1.5 Hz, 1H, CH$_{oxazine}$), 4.64 (s, 2H, CH$_{2oxazine}$), 4.42 (dd, J=14.0, 3.3 Hz, 1H, CH$_{2oxazine}$), 4.32 (d, J=12.9 Hz, 1H, CH$_{2oxazine}$), 3.28–3.24 (m, 4H, CH$_{2piperazine}$), 3.11–3.05 (m, 4H, CH$_{2piperazine}$). ^{13}C NMR (100 MHz, DMSO-d_6) δ: 153.4; 152.0; 150.9; 146.8; 142.1; 134.9 (d, J_{C-F}=10.9 Hz, 1 C); 133.9 (d, J_{C-F}=10.3 Hz, 1 C); 128.9 (2 C); 124.9; 119.6 (d, J_{C-F}=3.7 Hz, 1 C); 119.1; 117.9; 115.5 (2 C); 114.4; 106.6 (d, J_{C-F}=22.9 Hz, 1 C); 68.5; 62.7; 50.4; 48.4 (4 C); 47.0. MS/APCI m/z: calcd for C$_{23}$H$_{22}$ClFN$_6$O$_5$ 516.1, found: [M]$^-$ 516.0.

(*S*)-2-Nitro-6,7-dihydro-5*H*-imidazo[2,1-*b*][1,3]oxazin-6-yl (3-fluoro-4-(4-(pyridin-2-yl)piperazin-1-yl)phenyl)carbamate (52)

Off-white solid; yield 11%; mp: 211–214 °C; R$_f$=0.56 (EtOAc-*n*-hexane, 9:1). ^{1}H NMR (400 MHz, DMSO-*d6*) δ: 9.94 (s, 1H, NH$_{carbamate}$), 8.13 (ddd, J=4.9, 1.9, 0.6 Hz, 1H, CH$_{pyridine}$), 8.09 (s, 1H, CH$_{aromatic}$), 7.55 (ddd, J=8.9, 7.1, 2.0 Hz, 1H, CH$_{pyridine}$), 7.34 (d, J=14.7 Hz, 1H, CH$_{aromatic}$), 7.16 (d, J=7.8 Hz, 1H, CH$_{aromatic}$), 7.02 (t, J=9.3 Hz, 1H, CH$_{aromatic}$), 6.87 (d, J=8.7 Hz, 1H, CH$_{aromatic}$), 6.66 (dd, J=6.8, 5.1 Hz, 1H, CH$_{pyridine}$), 5.42 (d, J=1.4 Hz, 1H, CH$_{oxazine}$), 4.64 (s, 2H, CH$_{2oxazine}$), 4.42 (dd, J=14.0, 3.4 Hz, 1H, CH$_{2oxazine}$), 4.32 (d, J=13.7 Hz, 1H, CH$_{2oxazine}$), 3.64–3.59 (m, 4H, CH$_{2piperazine}$), 3.05–2.99 (m, 4H, CH$_{2piperazine}$). ^{13}C NMR (100 MHz, DMSO-*d6*) δ: 158.9; 155.9; 153.5 (d, J_{C-F}=2.8 Hz, 1 C); 152.0; 147.5; 146.8; 137.5; 135.0 (d, J_{C-F}=9.0 Hz, 1 C); 133.9 (d, J_{C-F}=12.4 Hz, 1 C); 119.7 (d, J_{C-F}=4.1 Hz, 1 C); 117.9; 114.3 (d, J_{C-F}=6.1 Hz, 1 C); 113.2; 107.1; 106.4; 68.5; 62.8; 50.2 (2 C); 47.0; 44.7 (2 C). MS/APCI m/z: calcd for C$_{22}$H$_{22}$FN$_7$O$_5$ 483.2, found: [M+Cl]$^-$ 518.3.

(*S*)-2-Nitro-6,7-dihydro-5*H*-imidazo[2,1-*b*][1,3]oxazin-6-yl (3-fluoro-4-(4-(pyrimidin-2-yl)piperazin-1-yl)phenyl)carbamate (53)

Off-white solid; yield 31%; mp: 212–215 °C; R$_f$=0.51 (EtOAc-*n*-hexane, 9:1). ^{1}H NMR (400 MHz, DMSO-*d6*) δ: 9.94 (s, 1H, NH$_{carbamate}$), 8.38 (d, J=4.7 Hz, 2H, CH$_{pyrimidine}$), 8.08 (s, 1H, CH$_{aromatic}$), 7.34 (d, J=14.4 Hz, 1H, CH$_{aromatic}$), 7.15 (d, J=8.5 Hz, 1H, CH$_{aromatic}$), 7.01 (t, J=9.3 Hz, 1H, CH$_{aromatic}$), 6.65 (t, J=4.7 Hz, 1H, CH$_{pyrimidine}$), 5.42 (d, J=1.5 Hz, 1H, CH$_{oxazine}$), 4.63 (s, 2H, CH$_{2oxazine}$), 4.42 (dd, J=14.0, 3.4 Hz, 1H, CH$_{2oxazine}$), 4.32 (d, J=14.1 Hz, 1H, CH$_{2oxazine}$), 3.89–3.84 (m, 4H, CH$_{2piperazine}$), 3.01–2.96 (m, 4H, CH$_{2piperazine}$). ^{13}C NMR (100 MHz, DMSO-*d6*) δ: 161.1; 157.9 (2 C); 155.9; 153.5; 152.0; 146.8; 134.9 (d, J_{C-F}=8.9 Hz, 1 C); 133.9 (d, J_{C-F}=11.2 Hz, 1 C); 119.8 (d, J_{C-F}=3.7 Hz, 1 C); 117.9; 114.3 (d, J_{C-F}=1.7 Hz, 1 C); 110.3; 68.5; 62.7; 50.3; 46.9; 43.3 (4 C). MS/APCI m/z: calcd for C$_{21}$H$_{21}$FN$_8$O$_5$ 484.2, found: [M+H]$^+$ 485.2.

(*S*)-2-Nitro-6,7-dihydro-5*H*-imidazo[2,1-*b*][1,3]oxazin-6-yl (3-fluoro-4-(4-(4-(trifluoromethyl)phenyl)piperazin-1-yl)phenyl)carbamate (54)

Off-white solid; yield 17%; mp: 245–249 °C; R$_f$=0.59 (EtOAc-*n*-hexane, 9:1). ^{1}H NMR (400 MHz, DMSO-*d6*) δ: 9.94 (s, 1H, NH$_{carbamate}$), 8.09 (s, 1H, CH$_{aromatic}$), 7.53 (d, J=8.8 Hz, 3H, CH$_{aromatic}$), 7.35 (d, J=14.6 Hz, 1H, CH$_{aromatic}$), 7.17 (d, J=8.2 Hz, 1H, CH$_{aromatic}$), 7.12 (d, J=8.8 Hz, 3H, CH$_{aromatic}$), 7.03 (t, J=9.3 Hz, 1H, CH$_{aromatic}$), 5.42 (d, J=1.5 Hz, 1H, CH$_{oxazine}$), 4.64 (s, 2H, CH$_{2oxazine}$), 4.42 (dd, J=14.0, 3.4 Hz, 1H, CH$_{2oxazine}$), 4.32 (d, J=13.7 Hz, 1H, CH$_{2oxazine}$), 3.44–3.40 (m, 4H, CH$_{2piperazine}$), 3.10–3.06 (m, 4H, CH$_{2piperazine}$). ^{13}C NMR (100 MHz, DMSO-*d6*) δ: 155.9; 153.4; 153.2; 152.0; 146.8; 134.7 (d, J_{C-F}=3.0 Hz, 1 C); 133.9 (d, J_{C-F}=9.6 Hz, 1 C); 126.3 (2 C); 126.2; 123.6; 119.7 (d, J_{C-F}=4.0 Hz, 1 C); 118.2; 117.9; 114.3 (d, J_{C-F}=32.3 Hz, 2 C); 106.7; 68.5;

62.8; 50.1; 47.1 (4 C). MS/APCI m/z: calcd for C$_{24}$H$_{22}$F$_4$N$_6$O$_5$ 550.2, found: [M+H]$^+$ 551.2, [M+Cl]$^-$ 585.1.

(*S*)-2-Nitro-6,7-dihydro-5*H*-imidazo[2,1-*b*][1,3]oxazin-6-yl (3-fluoro-4-(4-(5-(trifluoromethyl)pyridin-2-yl)piperazin-1-yl)phenyl)carbamate (55)

Off-white solid; yield 27%; mp: 222–225 °C; R$_f$=0.67 (EtOAc-*n*-hexane, 9:1). ^{1}H NMR (400 MHz, DMSO-*d6*) δ: 9.94 (s, 1H, NH$_{carbamate}$), 8.43 (d, J=0.9 Hz, 1H, CH$_{pyridine}$), 8.09 (s, 1H, CH$_{pyridine}$), 7.82 (dd, J=9.2, 2.5 Hz, 1H, CH$_{aromatic}$), 7.35 (d, J=14.7 Hz, 1H, CH$_{aromatic}$), 7.16 (d, J=8.0 Hz, 1H, CH$_{aromatic}$), 7.02 (t, J=8.1 Hz, 3H, CH$_{aromatic}$), 5.42 (d, J=1.5 Hz, 1H, CH$_{oxazine}$), 4.64 (s, 2H, CH$_{2oxazine}$), 4.42 (dd, J=14.0, 3.4 Hz, 1H, CH$_{2oxazine}$), 4.32 (d, J=13.9 Hz, 1H, CH$_{2oxazine}$), 3.80–3.75 (m, 4H, CH$_{2piperazine}$), 3.05–3.00 (m, 4H, CH$_{2piperazine}$). ^{13}C NMR (100 MHz, DMSO-d_6) δ: 160.1; 155.9; 154.3; 153.5; 152.0; 146.8; 145.2; 134.7 (d, J_{C-F}=9.2 Hz, 1 C); 134.5; 134.0 (d, J_{C-F}=11.9 Hz, 1 C); 119.8; 117.9; 114.3; 113.5; 106.4 (d, J_{C-F}=26.9 Hz, 1 C); 68.5; 62.8; 50.8; 50.1 (2 C); 47.0; 44.3 (2 C). MS/APCI m/z: calcd for C$_{23}$H$_{21}$F$_4$N$_7$O$_5$ 551.2, found: [M+H]$^+$ 552.2.

(*S*)-2-Nitro-6,7-dihydro-5*H*-imidazo[2,1-*b*][1,3]oxazin-6-yl (3-fluoro-4-(4-(methylsulfonyl)piperazin-1-yl)phenyl)carbamate (56)

Off-white solid; yield 22%; mp: 235–239 °C; R$_f$=0.68 (EtOAc-*n*-hexane, 9:1). ^{1}H NMR (400 MHz, DMSO-*d6*) δ: 9.95 (s, 1H, NH$_{carbamate}$), 8.09 (s, 1H, CH$_{aromatic}$), 7.34 (d, J=14.2 Hz, 1H, CH$_{aromatic}$), 7.16 (d, J=7.9 Hz, 1H, CH$_{aromatic}$), 7.02 (t, J=9.3 Hz, 1H, CH$_{aromatic}$), 5.42 (d, J=1.5 Hz, 1H CH$_{oxazine}$), 4.63 (s, 2H, CH$_{2oxazine}$), 4.42 (dd, J=14.0, 3.4 Hz, 1H, CH$_{2oxazine}$), 4.32 (d, J=14.4 Hz, 1H, CH$_{2oxazine}$), 3.27–3.22 (m, 4H, CH$_{2piperazine}$), 3.05–3.00 (m, 4H, CH$_{2piperazine}$), 2.92 (s, 3H, CH$_{3methylsulfonyl}$). ^{13}C NMR (100 MHz, DMSO-*d6*) δ: 155.9; 153.4; 152.0; 146.8; 134.4 (d, J_{C-F}=4.9 Hz, 1 C); 134.3 (d, J_{C-F}=6.1 Hz, 1 C); 120.0 (d, J_{C-F}=3.7 Hz, 1 C); 117.9 (d, J_{C-F}=2.1 Hz, 1 C); 114.3; 106.4 (d, J_{C-F}=27.6 Hz, 1 C); 68.5; 62.8; 49.9 (2 C); 46.9; 45.5 (2 C); 33.8. MS/APCI m/z: calcd for C$_{18}$H$_{21}$FN$_6$O$_7$S 484.1, found: [M+Cl]$^-$ 519.0.

Conflict of Interest

The authors declare no conflicts of interest.

ChemMedChem

Research Article
doi.org/10.1002/cmdc.202300015

Chemistry
Europe
European Chemical
Societies Publishing

Data Availability Statement

The data that support the findings of this study are available in the supplementary material of this article.

[1] T. Paulson, *Nature* **2013**, *502*, S2–S3.
[2] I. Hershkovitz, H. D. Donoghue, D. E. Minnikin, G. S. Besra, O. Y.-C. Lee, A. M. Gernaey, E. Galili, V. Eshed, C. L. Greenblatt, E. Lemma, G. K. Bar-Gal, M. Spigelman, *PLoS One* **2008**, *3*, e3426.
[3] World Health Organization, *Global Tuberculosis Report 2022*, Geneva, **2022**.
[4] World Health Organization, "WHO Coronavirus (COVID-19) Dashboard," can be found under https://covid19.who.int/, **2023**.
[5] G. F. S. Fernandes, A. M. Thompson, D. Castagnolo, W. A. Denny, J. L. Dos Santos, *J. Med. Chem.* **2022**, *65*, 7489–7531.
[6] C. Lange, K. Dheda, D. Chesov, A. M. Mandalakas, Z. Udwadia, C. R. Horsburgh-Jr, *Lancet* **2019**, *394*, 953–966.
[7] V. A. Dartois, E. J. Rubin, *Nat. Rev. Microbiol.* **2022**, *20*, 685–701.
[8] World Health Organization, *Meeting Report of the WHO Expert Consultation on the Definition of Extensively Drug-Resistant Tuberculosis*, Geneva, **2021**.
[9] G. Riccardi, I. G. Old, S. Ekins, *Drug Discovery Today* **2017**, *22*, 487–491.
[10] N. J. Ryan, J. H. Lo, *Drugs* **2014**, *74*, 1041–1045.
[11] S. J. Keam, *Drugs* **2019**, *79*, 1797–1803.
[12] M. Matsumoto, H. Hashizume, T. Tomishige, M. Kawasaki, H. Tsubouchi, H. Sasaki, Y. Shimokawa, M. Komatsu, *PLoS Med.* **2006**, *3*, e466.
[13] U. Manjunatha, H. I. M. Boshoff, C. E. Barry, *Commun. Integr. Biol.* **2009**, *2*, 215–218.
[14] A. Van den Bossche, H. Varet, A. Sury, O. Sismeiro, R. Legendre, J. Y. Coppee, V. Mathys, P. J. Ceyssens, *Tuberculosis* **2019**, *117*, 18–23.
[15] M. Dogra, B. D. Palmer, G. Bashiri, M. D. Tingle, S. S. Shinde, R. F. Anderson, R. O'Toole, E. N. Baker, W. A. Denny, N. A. Helsby, *Br. J. Pharmacol.* **2011**, *162*, 226–236.
[16] R. Singh, U. Manjunatha, H. I. M. Boshoff, Y. H. Ha, P. Niyomrattanakit, R. Ledwidge, C. S. Dowd, I. Y. Lee, P. Kim, L. Zhang, S. Kang, T. H. Keller, J. Jiricek, C. E. Barry, *Science* **2008**, *322*, 1392–1395.
[17] World Health Organization, *WHO Consolidated Guidelines on Drug-Resistant Tuberculosis Treatment*, Geneva, **2019**.
[18] World Health Organization, *Rapid Communication: Key Changes to the Treatment of Drug-Resistant Tuberculosis*, Geneva, **2022**.
[19] T. V. A. Nguyen, R. M. Anthony, A.-L. Bañuls, T. V. A. Nguyen, D. H. Vu, J. W. C. Alffenaar, *Clin. Infect. Dis.* **2018**, *66*, 1625–1630.
[20] W. He, C. Liu, D. Liu, A. Ma, Y. Song, P. He, J. Bao, Y. Li, B. Zhao, J. Fan, Q. Cheng, Y. Zhao, *J. Glob. Antimicrob. Resist.* **2021**, *26*, 241–248.
[21] S. Khoshnood, E. Taki, N. Sadeghifard, V. H. Kaviar, M. H. Haddadi, Z. Farshadzadeh, E. Kouhsari, M. Goudarzi, M. Heidary, *Front. Microbiol.* **2021**, *12*, 717045.
[22] G. F. S. Fernandes, P. C. De Souza, E. Moreno-Viguri, M. Santiváñez-Veliz, R. Paucar, S. Pérez-Silanes, K. Chegaev, S. Guglielmo, L. Lazzarato, R. Fruttero, C. M. Chin, P. B. Da Silva, M. Chorilli, M. C. Solcia, C. M. Ribeiro, C. S. P. Silva, L. B. Marino, P. L. Bosquesi, D. M. Hunt, L. P. S. De Carvalho, C. A. D. S. Costa, S. Cho, Y. Wang, S. G. Franzblau, F. R. Pavan, J. L. Dos Santos, *J. Med. Chem.* **2017**, *60*, 8647–8660.
[23] G. F. S. Fernandes, D. L. Campos, I. C. Da Silva, J. L. B. Prates, A. R. Pavan, F. R. Pavan, J. L. Dos Santos, *ChemMedChem* **2021**, *16*, 1268–1282.
[24] W. A. Denny, B. D. Palmer, *Future Med. Chem.* **2010**, *2*, 1295–1304.
[25] H. D. Showalter, *Molecules* **2020**, *25*, 4137.
[26] J. Cherian, I. Choi, A. Nayyar, U. H. Manjunatha, T. Mukherjee, Y. S. Lee, H. I. Boshoff, R. Singh, Y. H. Ha, M. Goodwin, S. B. Lakshminarayana, P. Niyomrattanakit, J. Jiricek, S. Ravindran, T. Dick, T. H. Keller, V. Dartois, C. E. Barry, *J. Med. Chem.* **2011**, *54*, 5639–5659.
[27] B. D. Palmer, A. M. Thompson, H. S. Sutherland, A. Blaser, I. Kmentova, S. G. Franzblau, B. Wan, Y. Wang, Z. Ma, W. A. Denny, *J. Med. Chem.* **2010**, *53*, 282–294.
[28] B. D. Palmer, H. S. Sutherland, A. Blaser, I. Kmentova, S. G. Franzblau, B. Wan, Y. Wang, Z. Ma, W. A. Denny, A. M. Thompson, *J. Med. Chem.* **2015**, *58*, 3036–3059.
[29] A. M. Thompson, P. D. O'Connor, A. J. Marshall, V. Yardley, L. Maes, S. Gupta, D. Launay, E. Chatelain, S. G. Franzblau, B. Wan, Y. Wang, Z. Ma, C. B. Cooper, W. A. Denny, *J. Med. Chem.* **2017**, *60*, 4212–4233.
[30] A. M. Thompson, H. S. Sutherland, B. D. Palmer, I. Kmentova, A. Blaser, S. G. Franzblau, B. Wan, Y. Wang, Z. Ma, W. A. Denny, *J. Med. Chem.* **2011**, *54*, 6563–6585.
[31] A. Blaser, B. D. Palmer, H. S. Sutherland, I. Kmentova, S. G. Franzblau, B. Wan, Y. Wang, Z. Ma, A. M. Thompson, W. A. Denny, *J. Med. Chem.* **2012**, *55*, 312–326.
[32] Rakesh, D. F. Bruhn, M. S. Scherman, A. P. Singh, L. Yang, J. Liu, A. J. Lenaerts, R. E. Lee, *Bioorg. Med. Chem. Lett.* **2016**, *26*, 388–391.
[33] A. Orita, K. Miwa, G. Uehara, J. Otera, *Adv. Synth. Catal.* **2007**, *349*, 2136–2144.
[34] A. M. Thompson, M. Bonnet, H. H. Lee, S. G. Franzblau, B. Wan, G. S. Wong, C. B. Cooper, W. A. Denny, *ACS Med. Chem. Lett.* **2017**, *8*, 1275–1280.
[35] A. M. Thompson, A. Blaser, R. F. Anderson, S. S. Shinde, S. G. Franzblau, Z. Ma, W. A. Denny, B. D. Palmer, *J. Med. Chem.* **2009**, *52*, 637–645.
[36] B. Xu, X. Ding, Y. Wu, L. Cui, P. Qian, D. Wang, Y. Zhao, *Chem. Res. Chin. Univ.* **2018**, *34*, 51–56.
[37] P. Xiang, T. Zhou, L. Wang, C. Y. Sun, J. Hu, Y. L. Zhao, L. Yang, *Molecules* **2012**, *17*, 873–883.
[38] J. C. Palomino, A. Martin, M. Camacho, H. Guerra, J. Swings, F. Portaels, *Antimicrob. Agents Chemother.* **2002**, *46*, 2720–2722.
[39] A. K. Ghosh, M. Brindisi, *J. Med. Chem.* **2015**, *58*, 2895–2940.
[40] F. R. Pavan, P. I. D. S. Maia, S. R. A. Leite, V. M. Deflon, A. A. Batista, D. N. Sato, S. G. Franzblau, C. Q. F. Leite, *Eur. J. Med. Chem.* **2010**, *45*, 1898–1905.
[41] G. F. S. Fernandes, P. C. De Souza, L. B. Marino, K. Chegaev, S. Gugliemo, L. Lazzarato, R. Fruttero, M. C. Chung, F. R. Pavan, J. L. Dos Santos, *Eur. J. Med. Chem.* **2016**, *123*, 523–531.
[42] C. J. Queval, R. Brosch, R. Simeone, *Front. Microbiol.* **2017**, *8*, 2284.
[43] S. Ehrt, D. Schnappinger, *Cell. Microbiol.* **2009**, *11*, 1170–1178.
[44] E. S. Zuniga, J. Early, T. Parish, *Future Microbiol.* **2015**, *10*, 217–229.
[45] M. Miyata, F. R. Pavan, D. N. Sato, L. B. Marino, M. H. Hirata, R. F. Cardoso, F. A. F. de Melo, C. F. Zanelli, C. Q. F. Leite, *Biomed. Pharmacother.* **2011**, *65*, 456–459.
[46] M. Piatek, G. Sheehan, K. Kavanagh, *Antibiotics* (Basel, Switzerland) **2021**, *10*, 1545.
[47] M. Varadi, S. Anyango, M. Deshpande, S. Nair, C. Natassia, G. Yordanova, D. Yuan, O. Stroe, G. Wood, A. Laydon, A. Žídek, T. Green, K. Tunyasuvunakool, S. Petersen, J. Jumper, E. Clancy, R. Green, A. Vora, M. Lutfi, M. Figurnov, A. Cowie, N. Hobbs, P. Kohli, G. Kleywegt, E. Birney, D. Hassabis, S. Velankar, *Nucleic Acids Res.* **2022**, *50*, D439–D444.
[48] S. E. Cellitti, J. Shaffer, D. H. Jones, T. Mukherjee, M. Gurumurthy, B. Bursulaya, H. I. Boshoff, I. Choi, A. Nayyar, Y. S. Lee, J. Cherian, P. Niyomrattanakit, T. Dick, U. H. Manjunatha, C. E. Barry, G. Spraggon, B. H. Geierstanger, *Structure* **2012**, *20*, 101–112.
[49] M. Gurumurthy, T. Mukherjee, C. S. Dowd, R. Singh, P. Niyomrattanakit, J. A. Tay, A. Nayyar, Y. S. Lee, J. Cherian, H. I. Boshoff, T. Dick, C. E. Barry III, U. H. Manjunatha, *FEBS J.* **2012**, *279*, 113–125.
[50] A. E. Mohamed, K. Condic-Jurkic, F. H. Ahmed, P. Yuan, M. L. O'Mara, C. J. Jackson, M. L. Coote, *Biochemistry* **2016**, *55*, 6908–6918.
[51] B. M. Lee, L. K. Harold, D. V. Almeida, L. Afriat-Jurnou, H. L. Aung, B. M. Forde, K. Hards, S. J. Pidot, F. H. Ahmed, A. E. Mohamed, M. C. Taylor, N. P. West, T. P. Stinear, C. Greening, S. A. Beatson, E. L. Nuermberger, G. M. Cook, C. J. Jackson, *PLoS Pathog.* **2020**, *16*, e1008287.
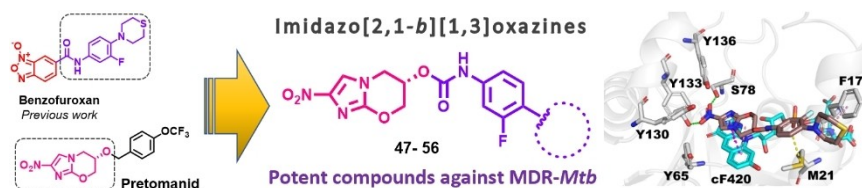[52] I. Rozas, I. Alkorta, J. Elguero, *J. Phys. Chem. A* **1998**, *102*, 9925–9932.

RESEARCH ARTICLE

Tackling tuberculosis resistance: A hit optimization campaign was performed to optimize a series of previously identified benzofuroxan derivatives. By switching benzofuroxan with the imidazo[2,1-*b*][1,3]oxazine subunit, we discovered a new series of leads with superior activity in inhibiting MDR-*Mtb in vitro* and intramacrophage mycobacterial growth. Furthermore, the new compounds did not show cytotoxicity against three cell lines or any toxicity to *Galleria mellonella*.

Dr. G. F. S. Fernandes*, K. F. Manieri, A. F. Bonjorno, Dr. D. L. Campos, Dr. C. M. Ribeiro, F. M. Demarqui, D. A. G. Ruiz, Prof. N. M. Nascimento-Junior, Prof. W. A. Denny, Dr. A. M. Thompson*, Prof. F. R. Pavan*, Prof. J. L. Dos Santos*

1 – 11

Synthesis and Anti-*Mycobacterium tuberculosis* Activity of Imidazo[2,1-*b*][1,3]oxazine Derivatives against Multidrug-Resistant Strains